

Article

Effects of the Gully Land Consolidation Project on Runoff and Peak Flow Rate on the Loess Plateau, China

Ge Wu^{1,2}, Suhua Fu^{1,3,4,*}, Guiyun Zhou⁵ and Chenguang Liu⁶

- ¹ State Key Laboratory of Soil Erosion and Dryland Farming on the Loess Plateau, Institute of Soil and Water Conservation, Chinese Academy of Sciences and Ministry of Water Resources, Xianyang 712100, China
- ² University of Chinese Academy of Sciences, Beijing 100049, China
- ³ School of Geography, Faculty of Geographical Science, Beijing Normal University, Beijing 100875, China
- ⁴ Beijing Key Laboratory of Environmental Remote Sensing and Digital Cities, Faculty of Geographical Science, Beijing Normal University, Beijing 100875, China
- ⁵ Center for Information Geoscience, University of Electronic Science and Technology of China, Chengdu 611731, China
- ⁶ Institute of Soil and Water Conservation, Northwest A & F University, Xianyang 712100, China
- * Correspondence: suhua@bnu.edu.cn

Abstract: The Gully Land Consolidation (GLC) project, aiming to create land for agriculture on the Loess Plateau, heavily interfered with the underlying surface and thus affected the hydrological process. The purpose of this study was to investigate the effects of the GLC on the surface runoff and peak flow rates of watershed on the Loess Plateau under different rainfall events and hydrological years. A GIS-based Soil Conservation Service Curve Number (SCS-CN) model was used. The results showed that GLC reduced the mean event surface runoff by 6.2–24.7%, and the reducing efficiency was the highest under light rain events. GLC also decreased annual surface runoff, and the reducing efficiency was 12.04% (normal year) > 7.63% (wet year) > 4.45% (dry year). In addition, GLC decreased the peak flow rate of the watershed by 8.1–30.2% and prolonged the time to peak flow rate. The efficiency of GLC in reducing the peak flow rate was higher under light rain events than that under extraordinary storm events. The reason for the decrease in runoff and peak flow rate after GLC was that the GLC decreased the slope gradient and hydrological connectivity of the watershed. The results will provide guidance for the application of GLC on the Loess Plateau and watershed management for similar regions.

Keywords: hydrological process; SCS-CN; slope gradient; hydrological connectivity; human activity



Citation: Wu, G.; Fu, S.; Zhou, G.; Liu, C. Effects of the Gully Land Consolidation Project on Runoff and Peak Flow Rate on the Loess Plateau, China. *Water* **2022**, *14*, 2582. <https://doi.org/10.3390/w14162582>

Academic Editor: Ataur Rahman

Received: 19 June 2022

Accepted: 15 August 2022

Published: 21 August 2022

Publisher's Note: MDPI stays neutral with regard to jurisdictional claims in published maps and institutional affiliations.



Copyright: © 2022 by the authors. Licensee MDPI, Basel, Switzerland. This article is an open access article distributed under the terms and conditions of the Creative Commons Attribution (CC BY) license (<https://creativecommons.org/licenses/by/4.0/>).

1. Introduction

China has launched several afforestation programs to restore local environment and mitigate climate change since 1978 [1] and is leading in greening the world [2]. Among these ecological programs, the Grain for Green (GFG) project initiated in 1999 is the largest one. During GFG, cropland on slopes steeper than 25° was converted into vegetated land on the Loess Plateau [3]. The new round of GFG was launched in 2014, planning to convert 2.8×10^4 km² of unfavorable cropland into vegetated land [4]. Converting sloping cropland into vegetated land has significantly reduced soil erosion on the Loess Plateau, because the soil erosion rate on vegetated land is much lower than that on sloping cropland, which can be up to 6.94×10^3 – 95.89×10^3 t km⁻² under extreme rainstorms [5]. In order to control soil erosion, 10.8% (4.83×10^4 km²) cropland on the Loess Plateau was converted into vegetated land from 2000 to 2008 [6]. Specially, 42% (3.0×10^3 km²) of cropland in Yan'an was converted [7]. Although such a huge reduction in cropland has mitigated serious soil erosion on the Loess Plateau, it has also led to regional food shortages, threatening local people's livelihoods [8]. In order to balance environmental protection and economic development, the Yan'an government on the one hand decided to fill gullies to create

cropland in channels, and on the other hand, they will consolidate the GFG's achievements by continuing to convert unfavorable cropland into vegetated land on slopes. The process of filling gullies to create land in channels is the so-called Gully Land Consolidation (GLC) project. The project was listed as a major national land remediation project by the government, with an investment of RMB 4.8 billion, aiming to create 4.0×10^4 km² of land for agriculture from 2011 to 2020 in places where it used to be gully channels [9]. GLC is one of the projects included in land consolidation. Historically, land consolidation is the first instrument for dealing with the conflict between man and land resource worldwide [10–12]. For example, the Zuiderzee tidal estuary in the Netherlands created 1650 km² of land for agriculture, recreation and urbanization by means of land consolidation [13]. Land consolidation is a complex systematic project with a broad definition, aiming to improve rural development and environmental protections [14]. Certain kinds of projects adopted in land consolidation are based on local natural conditions and stakeholders' willingness [15]. Land consolidation in Europe or Japan pays more attention to tenure readjustment [10, 16,17]. However, Yan'an is located in the loess hilly-gully region, where about 270,000 gullies are longer than 500 m [18]. Special management is required to reduce negative agricultural effects in such an area with a high density of gullies [19]. Leveling land by means of engineering constructions was adopted in complementing GLC: (a) removing soil from slopes on both sides of a channel, (b) compacting the excavated slopes into stepped structures with 4–5 layers [20], establishing slope protection engineering such as planting shrubs and grass, building fish scale pits on excavated slopes to prevent subsidence, tunneling and soil erosion, (c) using the soil removed from slopes to fill gullies and level the surface to make the bottom of gullies flat or become gentle slopes [18]. From 2013 to 2017, Yan'an increased new cropland by 78.49 km² by filling gullies [21]. GLC was seen as the inheritance and development of check dam on the Loess Plateau, which created land quickly by artificially filling up gullies instead of natural silting [22]. In fact, GLC is an upgraded version of check dam which pays more attention to water resource management. Spillways, dam systems, irrigation and drainage systems were usually established in the GLC area, helping to improve the efficiency of water use and control soil erosion [23]. GLC is of benefit to improving ecological and agricultural sustainability [15,24].

GLC adopted modern construction machinery to extract soil from slopes and use it to fill gullies to create flat land, during which the underlying surface of watershed was changed. However, local micro topography changed by land consolidation has caused hydrological process change [25]. Recent research has shown that GLC has affected the hydrological process. A laboratory study conducted by Lou et al. [26] found that both the volume and the velocity of runoff decreased as the ratios of the land consolidation area increased. Sun et al. [27] indicated that land consolidation could effectively replenish groundwater by retaining more surface runoff in gullies. Kang et al. [28] evaluated the effects of the GLC on runoff by the Soil and Water Assessment Tool (SWAT) model, and the results showed that river runoff decreased by 6.34–18.13% when the ratio of the GLC area to the watershed area increased from 0.23% to 0.91%. The results of Guo et al.'s [29] study showed that a thick loess layer on newly created land made it easier for surface ponding to occur, and a blind ditch was recommended to prevent salinization and swamping resulting from ponding. Zhao et al. [9] and Wang et al. [30] suggested that GLC had a profound impact on soil moisture content; one of the reasons was that the land created by GLC was flat and broad, and thus, the surface runoff was dispersed and redistributed more easily. In order to improve watershed management, it is necessary to evaluate the impact of GLC on the watershed hydrological process. The assessment of GLC's hydrological impact should be based on hydrological situation, i.e., rainfall characteristics [10]. Studies showed that the proportion of runoff and runoff reduction caused by different rainfall characteristics varied [31–34]. However, the relationship between rainfall and GLC's hydrological impact has not been fully studied yet. In order to fill the research gap, a GIS-based SCS-CN model was developed in this study to investigate the changes of surface runoff and peak flow rate before and after the implementation of GLC. The results will provide guidance for

watershed management and the implementation of the GLC on the Loess Plateau and other similar regions.

2. Materials and Methods

2.1. Study Area

Xingshuyaozi watershed ($36^{\circ}35'13''$ – $36^{\circ}33'51''$ N, $109^{\circ}18'56''$ – $109^{\circ}17'25''$ E) is located in Yan'an, Shaanxi Province, located on the central Loess Plateau, China (Figure 1). The watershed covers an area of 3.72 km^2 . The soil is formed based on loess parent materials and was classified as sandy clay loam [35]. The study area has a typical hilly-gully landscape and drains directly into the Yanhe River. The elevation of the watershed ranges from 1120 m to 1380 m. It has typical continental characteristics and belongs to the semi-arid continental climatic zone [36]. According to precipitation data collected from Baota station, the average annual precipitation from 1951 to 2019 was 533 mm. The precipitation in July, August and September accounts for approximately 70% of the annual precipitation.

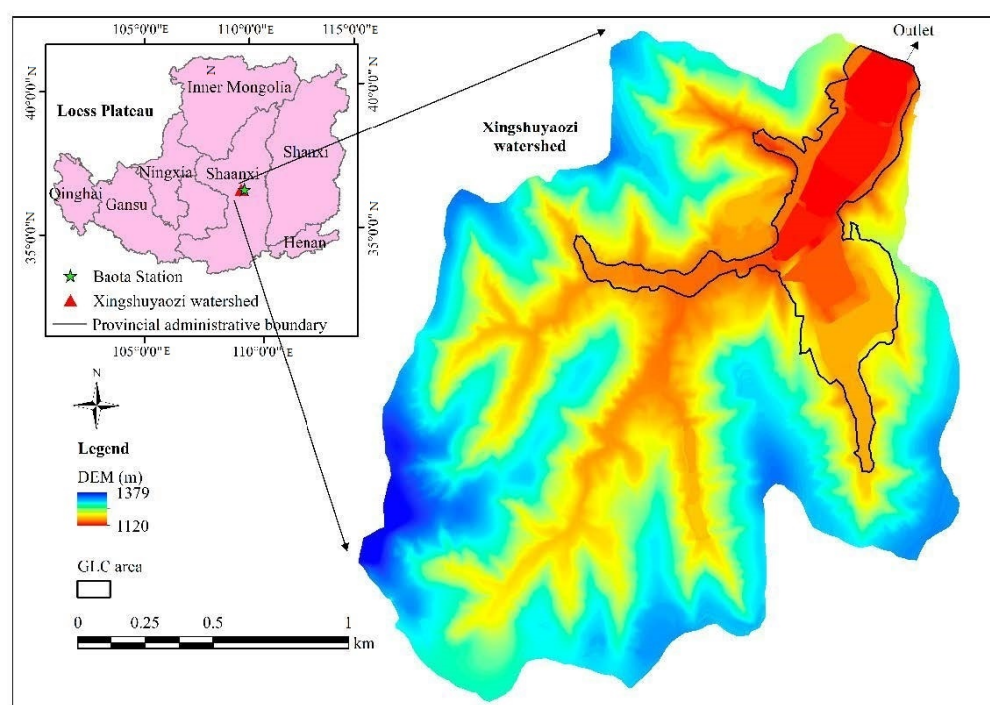


Figure 1. Location and the DEM after GLC (in 2019) of Xingshuyaozi watershed.

The GLC in Xingshuyaozi watershed was conducted from 2015 to 2018. The GLC area covers an area of 0.39 km^2 , accounting for 10.36% of the watershed area (Figure 1). It used to be a mosaic of cropland, shrub and grassland at the bottom and both sides of the gully. GLC integrated the previously scattered and sporadic cultivated land in the gully into the newly created land at the bottom of the gully, forming a centralized and contiguous new cultivated land. GLC facilitated mechanization and large-scale operation in local agriculture industry. Land use in Xingshuyaozi watershed before and after the implementation of GLC is shown in Figure 2. Before GLC, forestland, cropland, shrub, grassland, orchard and others accounted for 51.9%, 8.0%, 13.0%, 10.5%, 13.2% and 3.4%, respectively. After GLC, forestland, cropland, shrub, grassland, orchard and others account for 52.0%, 9.5%, 10.8%, 10.9%, 13.2% and 3.6%.

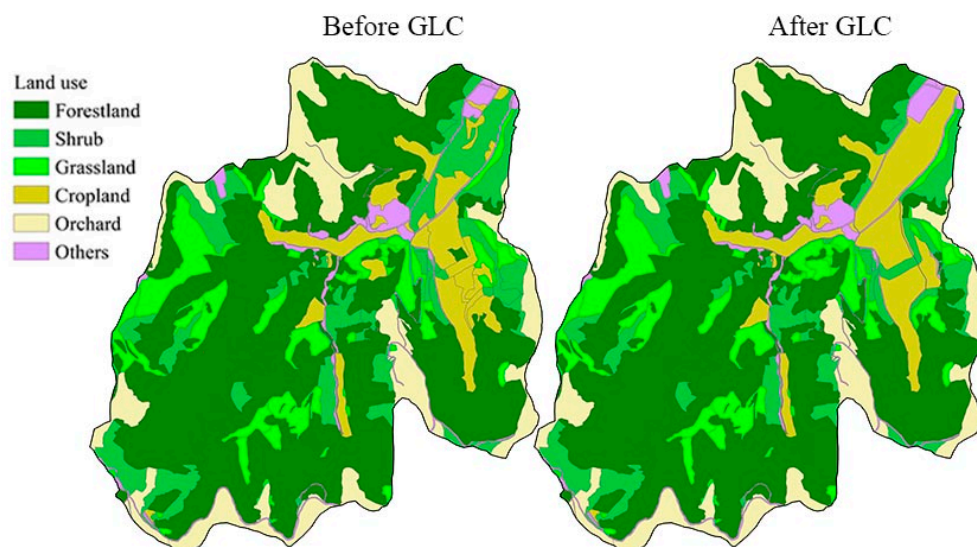


Figure 2. Land use in Xingshuyaozi watershed before GLC (in 2013) and after GLC (in 2019).

GLC in Xingshuyaozi watershed was conducted by excavating slopes on both sides of the gully, filling the excavated soil into the bottom of the gully, then making the gully bottom flat and wide. The excavated slopes, with a slope gradient of about 50° , were protected by interception drain, vegetation and fish scale pits.

2.2. Data Sources

The land use maps of the watershed are shown in Figure 2. Land use and soil conservation maps were produced by interpreting remote sensing images of the watershed. A field survey was carried out to verify the interpreted land use and soil conservation maps. The remote sensing images before the GLC and after the GLC were downloaded from Google Earth with a resolution of 0.5 m (Figure 3).

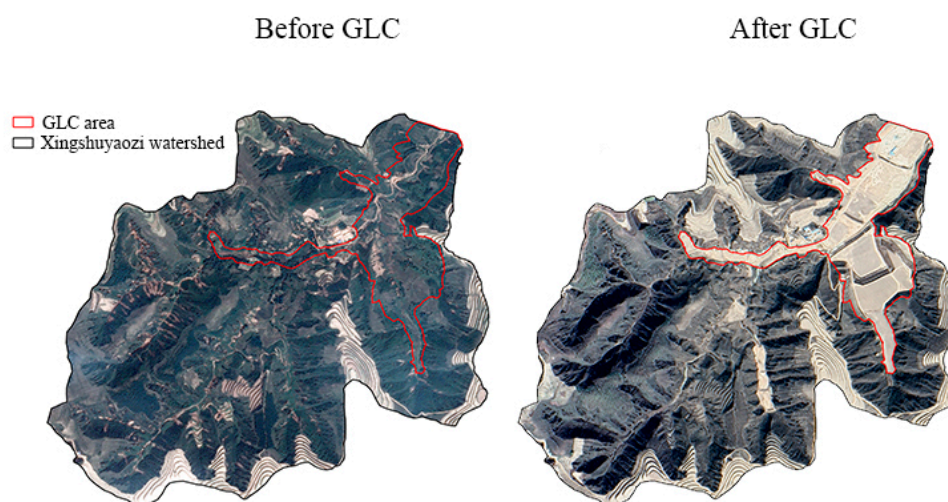


Figure 3. Remote sensing images of Xingshuyaozi watershed before GLC (in 2013) and after GLC (in 2019).

An auto-recording tipping bucket rain gauge and a radar water level sensor were installed at the outlet of the Xingshuyaozi watershed in 2018 to measure and record the rainfall amount and water level, respectively (Figure 4). Hydraulic radius and channel slope were measured and calculated during field investigation. The precipitation data from 1951 to 2019 at the Baota station (Figure 5) were used to determine the typical hydrological years of the Xingshuyaozi watershed. The Baota station is the closest national weather station to Xingshuyaozi watershed, which is approximately 10 km away from it (Figure 1).

Pearson-III curve method was used to determine typical wet year, normal year and dry year with a probability of 25%, 50% and 75%, respectively [37]. According to the result of Pearson-III analysis, the years 1981, 1971 and 1974 were chosen as typical wet year, normal year and dry year, respectively. Annual precipitation of the years 1981, 1971 and 1974 was 774 mm, 456 mm and 330 mm, respectively. The 40 rainfall events in 1981, 1971 and 1974 were divided into light rain, moderate rain, heavy rain, rainstorm and extraordinary storm based on the 24 h rainfall amount, according to the standard issued by the China Meteorological Administration (CMA) (Table 1) [38]. Among the 40 rainfall events, there were 4 light rain events, 21 moderate rain events, 11 heavy rain events, 3 rainstorm events and 1 extraordinary storm events.



Figure 4. The auto-recording tipping bucket rain gauge and radar water level sensor at watershed outlet.

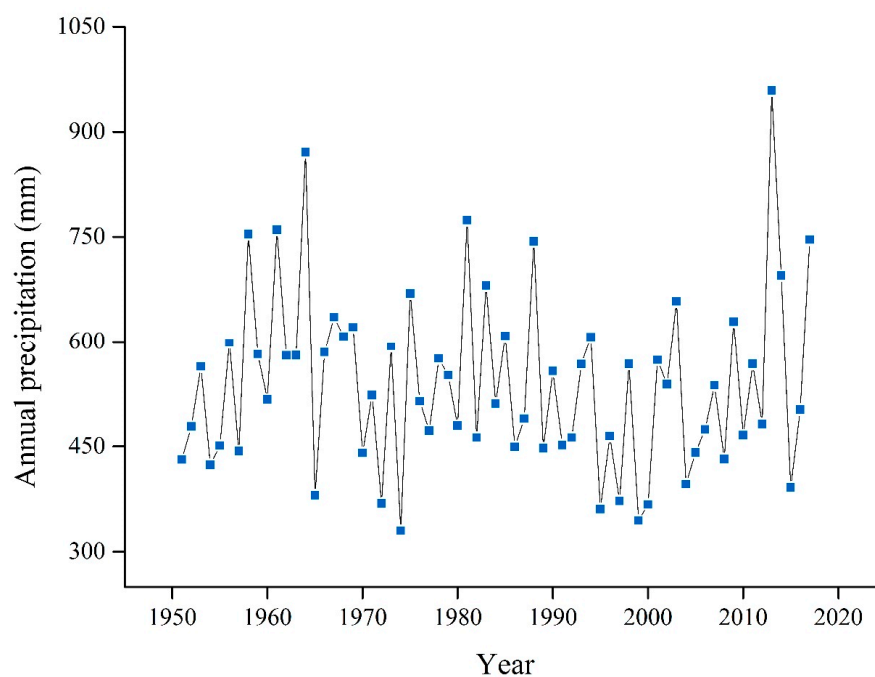


Figure 5. Annual precipitation from 1951 to 2019 at Baota Station.

Table 1. The standard of rainfall levels.

Precipitation (mm)	$P < 10$	$10 \leq P < 25$	$25 \leq P < 50$	$50 \leq P < 100$	$P \geq 100$
Level	Light rain	Moderate rain	Heavy rain	Rainstorm	Extraordinary storm

The 10 m digital elevation model (DEM) before GLC (in 2013) was derived from a 1:10,000 topographic map. The DEM after GLC (in 2019) was based on aerial survey topographic drawings.

2.3. Surface Runoff and Peak Flow Rate Simulation

A GIS-based SCS-CN method was established to estimate surface runoff in Xingshuyaozi watershed. The SCS-CN method was developed by the United States Department of Agriculture's Agricultural Research Service (USDA-ARS). Due to its simplicity and few data requirements, SCS-CN has been widely used in estimating runoff in small watershed for water resource management [39–47]. This methodology has also been used in many hydrological models [48], such as the SWAT [49] and the Chemicals, Runoff, and Erosion from Agricultural Management Systems model (CREAMS) [50]. In the 1990s, the SCS-CN method was introduced to China; since then, it has been widely used to estimate runoff from small watershed on the Loess Plateau [51–54]. The GIS-based SCS-CN method calculate runoff in a cell using Equations (1) and (2) [55]:

$$RO = (P_r - 0.2S)^2 / (P_r + 0.8S), P_r - 0.2S \geq 0 \quad (1)$$

$$RO = 0, P_r - 0.2S < 0 \quad (2)$$

where RO is the surface runoff depth in a cell (mm), P_r is the total rainfall amount in the cell (mm) and S is the soil storage capacity (mm). Soil storage capacity is related to soil type, land use and so on. In the SCS-CN method, S and CN are calculated using Equation (3) [56]:

$$CN = 25400 / (S + 254) \quad (3)$$

where CN is a dimensionless runoff index related to land use and hydrologic soil groups. According to the criteria of the classification of hydrologic soil groups (HSGs) [37], Xingshuyaozi watershed belongs to HSG B. The value of CN ranges from 0 to 100, and its value given by SCS table is for average antecedent moisture condition only [55]. The antecedent moisture condition (AMC) of the watershed was classified as dry conditions (AMC I), average conditions (AMC II) and wet conditions (AMC III) according to the 5-day antecedent rainfall amount.

CN for AMC I, AMC II and AMC III are CN_1 , CN_2 and CN_3 , respectively. CN_1 and CN_3 can be calculated with CN_2 using the equations [57]:

$$CN_1 = CN_2 - 20(100 - CN_2) / \{100 - CN_2 + \exp[2.533 - 0.0636(100 - CN_2)]\} \quad (4)$$

$$CN_3 = CN_2 \cdot \exp[0.00673 \cdot (100 - CN_2)] \quad (5)$$

Routing flow overland and in channels were described by the SCS unit hydrograph method [58] and Muskingum method [37], respectively.

Routing flow overland:

Since the average slope gradient in Xingshuyaozi watershed is over 10° , the peak flow rate was simulated with the equation given by Fu et al. [59]:

$$Q_{pout} = 6.69 \left(a_{out} / 10^6 \right)^{0.59} RO_{out}^{1.15(a_{out}/10^6)^{0.06}} P_{out}^{-0.72} \quad (6)$$

where Q_{pout} is the peak flow rate (m^3/s), a_{out} is the watershed area (km^2), RO_{out} is the surface runoff depth (mm) and P_{out} is the average rainfall amount above the cell's outlet (mm).

The time to peak flow rate was calculated by:

$$T_{pout} = 0.375 \cdot d_{urin} \quad (7)$$

$$d_{urin} = 2 \cdot \frac{a_{out} \cdot RO_{avout}}{Q_{pout} \cdot 1000} \quad (8)$$

where T_{pout} is the time to peak flow rate (min), RO_{avout} is the average surface runoff depth in a cell (mm). Then, the unit hydrograph can be estimated according to the table of ratios for dimensionless unit hydrograph and mass curve, provided by Chapter 16 in the *National Engineering Handbook* [60].

Routing flow in channels: the routing equation for the Muskingum method and the coefficients of C_1 , C_2 , C_3 are expressed as follows:

$$Q_{j+1} = C_1 I_{j+1} + C_2 I_j + C_3 Q_j, j = 1, 2, 3 \dots n \quad (9)$$

C_1 , C_2 and C_3 are coefficient calculated as:

$$\begin{aligned} C_1 &= \frac{\Delta t - 2 \cdot K_r \cdot X}{2 \cdot K_r \cdot (1 - X) + \Delta t} \\ C_2 &= \frac{\Delta t + 2 \cdot K_r \cdot X}{2 \cdot K_r \cdot (1 - X) + \Delta t} \\ C_3 &= \frac{2 \cdot K_r \cdot (1 - X) - \Delta t}{2 \cdot K_r \cdot (1 - X) + \Delta t} \end{aligned} \quad (10)$$

$$2K_r \cdot \Delta t < \Delta t < 2K_r \cdot (1 - X)$$

where Q_{j+1} is the outflow at $(j+1)$ th Δt , Δt is the time interval and here it was set as 20 min, K_r represents the travel time of the flood wave through the channel reach and here it was set as 50 min, X is a weighting factor depends on the shape of the modeled wedge storage and here it was set as 0.3.

2.4. Model Calibration and Validation

The measured rainfall and runoff data in 2019 (i.e., after GLC) were used to calibrate the model. The data in 2020–2021 were used to validate the model. The Nash–Sutcliffe efficiency (NSE) [61] and the ratio of the root mean square error to the standard deviation of measured data (RSR) [62] were used to evaluate the accuracy of the simulated surface runoff and peak flow rate.

The equations for the NSE and RSR are as follows:

$$NSE = 1 - \frac{\left[\sum_{i=1}^n (Y_i^{obs} - Y_i^{sim})^2 \right]}{\left[\sum_{i=1}^n (Y_i^{obs} - Y^{mean})^2 \right]} \quad (11)$$

$$RSR = \frac{RMSE}{STDEV_{obs}} = \frac{\sqrt{\sum_{i=1}^n (Y_i^{obs} - Y_i^{sim})^2}}{\sqrt{\sum_{i=1}^n (Y_i^{obs} - Y^{mean})^2}} \quad (12)$$

where Y_i^{obs} is the i th measured data, Y_i^{sim} is the i th simulated data, Y^{mean} is the average of measured data, $RMSE$ is the roof mean square error between measured data and simulated data, and $STDEV_{obs}$ is the standard deviation of measured data. After calibration and validation, the model was used to simulate the runoff depth and peak flow rate for the watershed. A paired T-test was used to show whether the GLC affected the runoff and peak flow rate significantly. The statistical analysis was conducted using the software program SPSS ver. 26.0 (SPSS Inc., Chicago, IL, USA).

The runoff or peak flow rate reduction efficiency is represented by the relative difference, which is calculated using Equation (13):

$$\Delta y = (x_a - x_b) / x_b \times 100\% \quad (13)$$

where Δy is the relative difference in runoff or peak flow rate after the GLC, x_a is the surface runoff or peak flow rate after the GLC, and x_b is the runoff or peak flow rate before the GLC. A negative Δy means that the surface runoff or peak flow rate decreases after the GLC, while a positive Δy means that the surface runoff or peak flow rate increases after the GLC.

2.5. Hydrological Connectivity

Hydrological connectivity refers to the water-mediated transfer of matter, energy or organisms within or between elements in a hydrological process [63]. Hydrological connectivity demonstrates pathways of flow between the landscape patterns. It was used to evaluate the effect of the GLC on runoff and peak flow rate. The hydrological connectivity was calculated according to the definition provided by Bracken and Croke [64].

3. Results

3.1. The Results of Calibration and Validation

The measured rainfall and runoff data of Xingshuyaozi watershed in 2019 (Table 2) were used to calibrate the CN values. Based on soil and water conservation measures, land use and HSG B, the CN values were calibrated and selected by trial and error until the model yield performed the best. The scatter plots of the measured data and the estimated data using the calibrated CN values are shown in Figure 6. Larger scatter was found in Figure 6b. This was because the peak flow rate was affected by rainfall amount, rainfall intensity and antecedent soil moisture, and runoff, etc. The runoff was simulated by SCS-CN, which could not consider the effect of rainfall intensity on runoff. In the equation for calculating peak flow rate, the effect of rainfall intensity was ignored, which may result the error. The NSE and RSR for runoff were 0.69 and 0.56. The NSE and RSR for the peak flow rate were 0.62 and 0.61. According to Moriasi et al. [65], the accuracy of simulation is accepted if $NSE > 0.50$ and $RSR \leq 0.70$. So, the calibration results indicated that the model fitted the measured runoff and peak flow rate data well.

Table 2. Measured rainfall and runoff at watershed outlet in 2019.

Date	Precipitation (mm)	Rainfall Intensity (mm/h)	Measured Runoff (mm)	Measured Peak Flow Rate (m ³ /s)	Measured Time to Peak Flow Rate (min)
21 July 2019	63	4.27	0.31	0.32	140
1 August 2019	75.5	41.18	11.16	16.46	160
3 August 2019	54.5	2.15	4.61	5.57	630
19 August 2019	38	1.43	1.31	0.19	540
27 August 2019	70	5.03	8.74	6.07	210
12 September 2019	47	2.15	2.24	0.65	420
5 October 2019	32	1.72	0.91	0.09	660

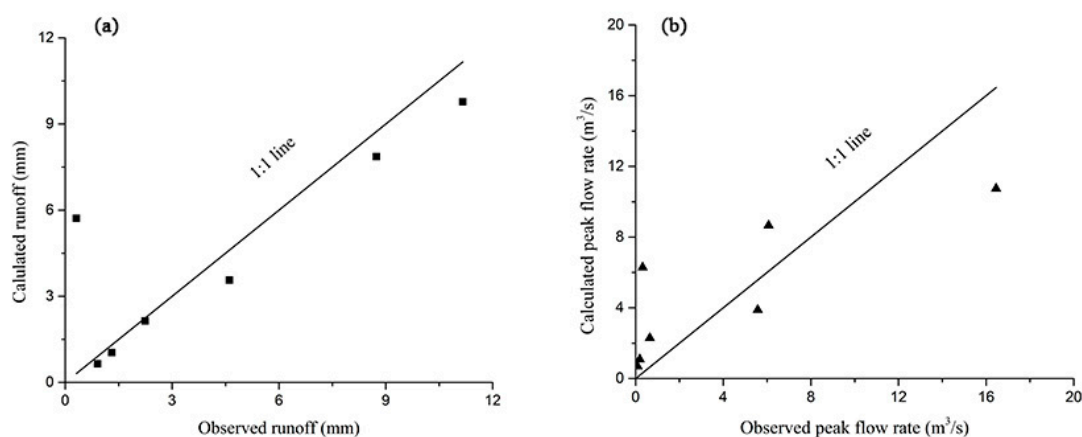


Figure 6. Scatter diagrams between observed and calibrated runoff (a) and peak flow rate (b).

In order to validate the model calibration, the measured rainfall and runoff of Xingshuyaozi in 2020 and 2021 were used. The measured and the validated data were close to the 1:1 line (Figure 7). The NSE and RSR were 0.96 and 0.20 for runoff, 0.77 and 0.47 for peak flow rate, respectively, indicating that the calibrated CN values worked well for Xingshuyaozi watershed.

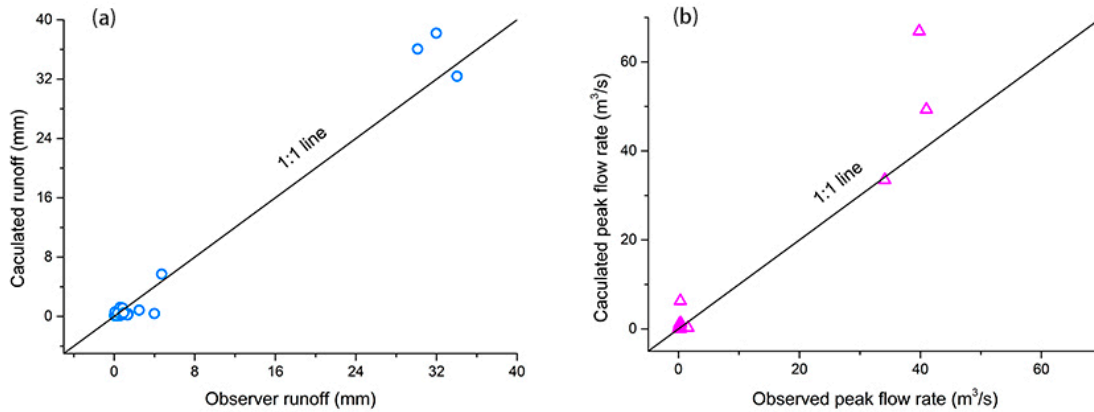


Figure 7. Scatter diagrams between observed and validated runoff (a) and peak flow rate (b).

3.2. Simulated Surface Runoff

The calibrated CN values were used to calculate surface runoff. The paired T-test showed that the estimated event surface runoff before and after GLC was different at a significance level of 0.05 (Table 3).

Table 3. Effects of the GLC on hydrological variables based on paired T-tests.

Variable	N	T Value	Sig.
RO	40	−3.66	0.001
T _p	40	17.00	0.000
Q _p	40	−4.29	0.000

Note: N is the number of rainfall events; RO is the runoff depth (mm); T_p is the time to peak flow rate (min); Q_p is the peak flow rate (m³/s).

The estimated mean event surface runoff depth is shown in Table 4. The mean event surface runoff depth ranged from 0.71 mm to 45.80 mm before GLC and ranged from 0.53 mm to 42.41 mm after GLC, respectively. Surface runoff increased with rainfall levels, i.e., the higher the rainfall level, the deeper the runoff depth. The reduction of surface runoff ranged from 0.06 mm to 3.39 mm after GLC, and the relative reduction ranged from 6.2% to 24.7% (Table 4). The highest efficiency of GLC at reducing runoff was found under light rain events, with a relative reduction of 24.7%. The lowest efficiency of GLC in reducing runoff was found under heavy rain events and the extraordinary storm event, with a relative reduction of 6.2–7.4%.

Table 4. The mean event surface runoff before and after the implementation of GLC.

Rainfall Levels	N	Mean Event Runoff (mm)			
		Before GLC	After GLC	Absolute Difference (mm)	Relative Difference (%)
Light rain	4	0.71	0.53	−0.17	−24.7
Moderate rain	21	0.76	0.68	−0.06	−10.4
Heavy rain	11	8.01	7.51	−0.49	−6.2
Rainstorm	3	5.55	4.47	−1.09	−19.6
Extraordinary storm	1	45.80	42.41	−3.39	−7.4

Note: N is the number of rainfall events.

Estimated annual surface runoff in typical hydrological years before and after GLC is shown in Figure 8. The annual runoff depth in wet year, normal year and dry year was

132.10 mm, 35.92 mm and 1.30 mm before the GLC, and 122.03 mm, 31.59 mm and 1.25 mm after the GLC, respectively. The efficiency of GLC at reducing annual surface runoff was 12.04% (normal year) > 7.63% (wet year) > 4.45% r (dry year), respectively.

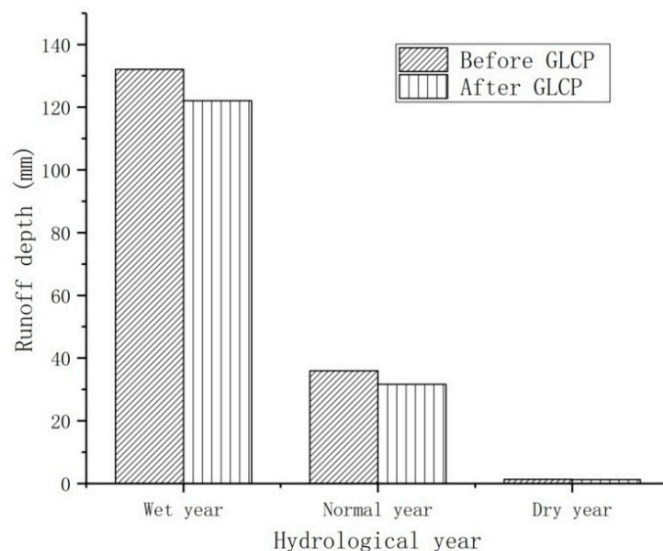


Figure 8. Annual surface runoff in different hydrological years before GLC (in 2013) and after GLC (in 2019).

The most obvious effect of GLC in reducing the surface runoff was found for light rain events, however, the effect of GLC in reducing annual surface runoff was the least for dry year, which seem to conflict with each other. In fact, this was because the rainfall events that occurred in the dry year were not necessarily light rainfall events. For example, seven moderate rains occurred in the dry year (Table 5).

Table 5. The number of different rainfall levels in wet year, normal year and dry year.

Rainfall Level	Wet Year	Normal Year	Dry Year
Light rain	3	1	0
Moderate rain	9	5	7
Heavy rain	7	4	0
Rainstorm	1	2	0
Extraordinary storm	1	0	0

3.3. Estimated Peak Flow Rate

The peak flow rate decreased significantly at a significance level of 0.05 after GLC (Table 3). The highest efficiency of GLC in reducing the peak flow rate was found under light rainfall events, with a relative reduction of 30.2%. Under moderate rain events and rainstorm events the efficiency of reducing the peak flow rate was 14.0% and 24.4%, respectively. The lowest efficiency of GLC in reducing the peak flow rate was found under heavy rain and extraordinary storm events, with a reduction of 8.1–10.1% (Table 6). It is obvious that the effect of GLC on peak flow rate is relatively small under extraordinary storm events.

Table 6. Peak flow rate before and after the implementation of GLC.

Rainfall Levels	N	Mean Event Peak Flow Rate (m ³ /s)			
		Before GLC	After GLC	Absolute Difference (m ³ /s)	Relative Difference (%)
Light rain	4	2.02	1.41	−0.61	−30.2
Moderate rain	21	1.75	1.51	−0.25	−14.0
Heavy rain	11	16.27	14.95	−1.31	−8.1
Rainstorm	3	6.47	4.89	−1.58	−24.4
Extraordinary storm	1	47.46	42.66	−4.80	−10.1

Note: N is the number of rainfall events.

In addition, the time to peak flow rate (T_p) was significantly prolonged after the GLC (Table 3). Figure 9 showed that the T_p ranged from 0 min to 520 min before the GLC, and from 280 min to 920 min after GLC. The T_p was prolonged 2–4 times after GLC.

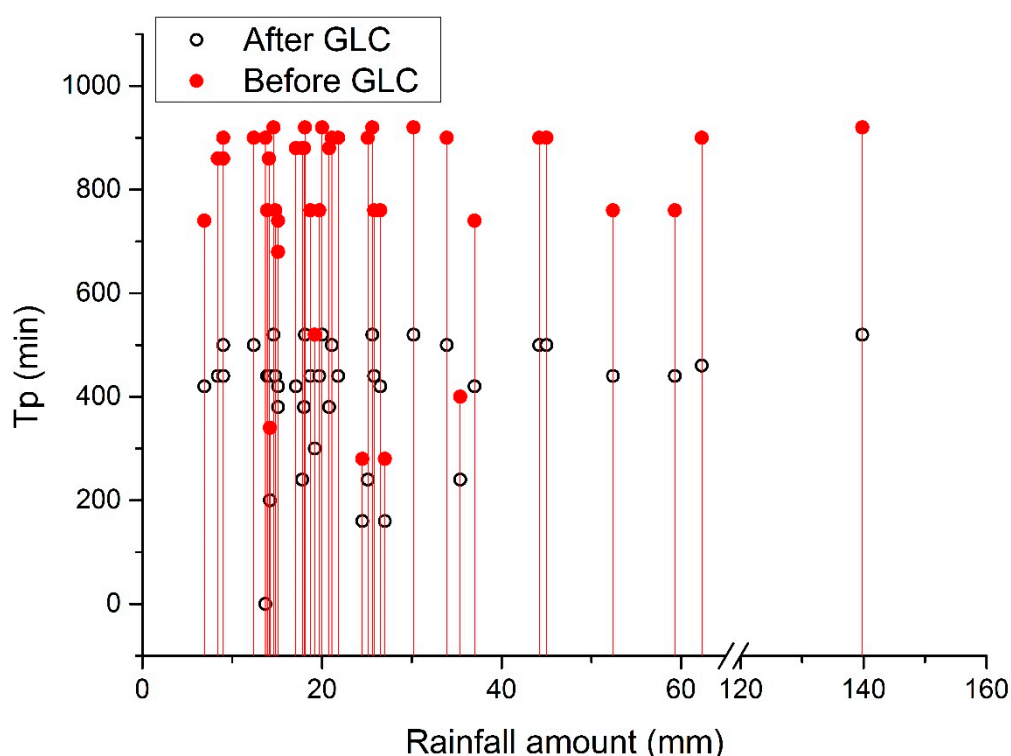


Figure 9. Time to the peak flow rate (T_p) before GLC (in 2013) and after GLC (in 2019).

4. Discussion

4.1. GLC Reduced Surface Runoff

The results of the study demonstrate that the GLC has decreased surface runoff depth. This conclusion confirms previous studies by Sun et al. [27] and Lou et al. [26] and more recently Kang et al. [28] and Ji et al. [66]. A possible explanation is that GLC decreased slope gradients in the watershed. Figure 10 illustrates the slope gradients of Xingshuyaozi watershed. The area with a slope gradient lower than 5° was obviously increased after GLC, indicating that the watershed became flatter than before. In the GLC area, cropland, grassland, shrub and others were mainly concentrated on slopes between 5° and 25°, over 35°, between 20° and 25° or over 35°, over 35° before GLC, respectively (Figure 11). However, cropland, grassland, shrub and others were mainly concentrated on slopes under 5° after GLC. Since the area of cropland under 5° after GLC accounted for 59.3%, much higher than any other land use types, it was marked by a blue frame. The average surface runoff in different land use decreased with a reduction ranging from 0.4% to 48.4% (Table 7). The reduction of surface runoff was significant at a significance level of 0.05 in cropland, forestland, grassland, shrub and others. Particularly in cropland, there was a reduction

of 48.4% in runoff after GLC. Runoff has been observed to decrease with a decrease in slope gradients [67,68]. Continuous monitoring of plots on the Loess Plateau under natural rainfall from 2015 to 2019 showed that annual runoff decreased by 48–207% when the slope gradient was reduced from 20° to 5° [69]. Lower slopes have a stronger ability to retain water than steeper slopes, and thus the surface runoff depth increases on lower slopes [68,70]. Increased runoff depth on the slope enhances the hydrological efficiency of flows [71], leading to an increase in infiltration rate. Therefore, decreased slope gradients should be the main reason for decreased runoff after GLC, which lead to a longer residence time of runoff on the slope and a higher infiltration rate. This speculation is reasonable since studies have shown that the water content in deep soil has increased and the ground water table has risen after the GLC [9,72,73], which indicate that GLC promotes more rainfall infiltrating the ground instead of leaving as surface runoff.

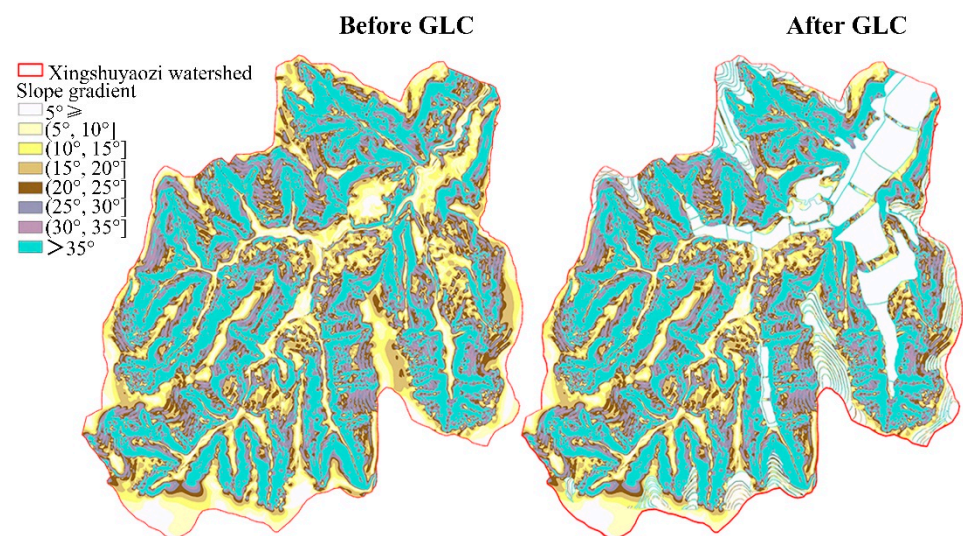


Figure 10. Slope gradient in Xingshuyaozi watershed before GLC (in 2013) and after GLC (in 2019).

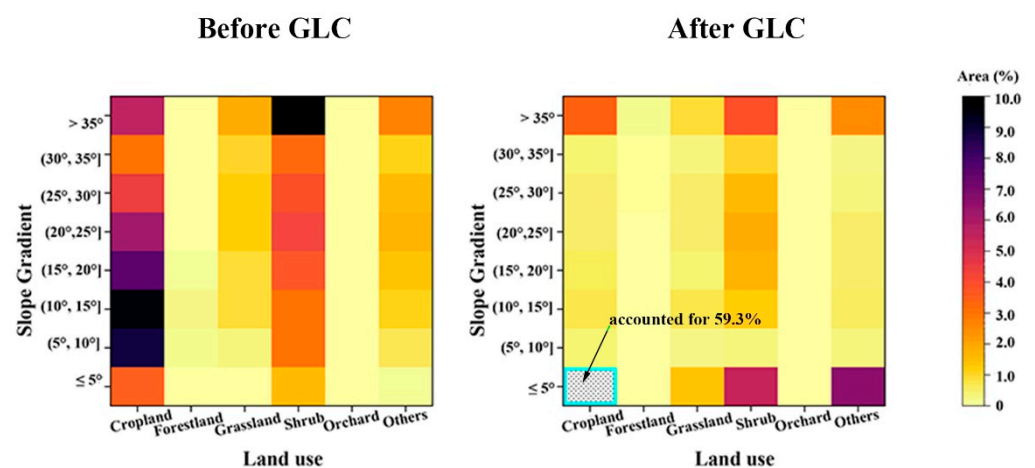


Figure 11. Land use and slope gradients in GLC area before and after the implementation of GLC. Note: Since the area of cropland with a slope gradient under 5° accounted for 59.3% after GLC, which is much higher than any other land use types, it was marked by a blue frame.

Table 7. Surface runoff in different land use types.

Land Use	N	T Value	Sig.	Mean Event Runoff (mm)			
				Before GLC	After GLC	Absolute Difference	Relative Difference (%)
Cropland	40	−3.69	0.001	7.87	4.06	−3.80	−48.4
Forestland	40	−3.22	0.003	3.48	3.47	−0.02	−0.4
Grassland	40	−3.38	0.002	5.38	5.17	−0.20	−3.8
Shrub	40	−4.09	0.000	4.41	4.12	−0.28	−6.4
Orchard	40	−2.17	0.037	2.31	2.28	−0.03	−1.3
Others	40	−3.96	0.000	11.06	10.60	−0.46	−4.2

Note: N means the number of rainfall events. The significant level of paired T-test is 0.05.

However, Bronstert et al. [10] found that average runoff in the consolidated watershed was 28% more than the non-consolidated watershed, which had a similar topography and the same soil as in Germany. Evrard et al. [74] also suggested that land consolidation led to an increase in peak flow and runoff volume. The results contradicted the current study. This is because the land consolidation procedures in watersheds mentioned by Bronstert et al. [10] and Evrard et al. [74] were mainly conducted to enlarge individual field size by removing small structures such as embankments, solitary trees and putting land units together without changing watershed slope gradients. These small structures are effective at holding back surface runoff on arable land, and the removal of them led to increased runoff production after land consolidation. In addition, the hydrological functioning of land consolidation depends on the scale of land consolidation and their location [75], so the effects of land consolidation might be diverse. Long-term perspective and data records about the changes in magnitude and timing of flow at the regional scale are required to provide insight into hydrological responses to anthropogenic activities.

4.2. GLC Reduced the Peak Flow Rate

The current study shows that GLC has decreased the peak flow rate and prolonged the time to peak flow rate. Ji et al. [66] also obtained a similar result. In general, the peak flow rate has a positive relationship with the slope gradient, and the time to peak flow rate has a negative relationship with the slope gradient. For example, in the equation for peak flow rate in the CREAMS model, there is an exponentially increasing relationship between slope and peak flow rate [76]. The equation developed for peak flow rate estimation by Liu et al. [77] also showed that peak flow rate was significantly correlated with slope steepness. Therefore, it is reasonable that the peak flow rate decreased after the GLC, during which the slope gradient of the watershed decreased. The time to peak flow rate becoming longer after the GLC can be explained from two aspects. First, a decreased slope gradient reduced the impact of gravity along the slope direction, so the velocity of runoff decreased [78,79]. Hessel et al. [80] also found that the time to peak flow rate simulated by the LISEM (Limburg soil erosion model) based on a DEM with a larger grid cell size increased, since the slope gradient derived from the DEM decreased as the grid cell size increased. Decreased slope gradient lowered the runoff velocity and energy [81]. Lower velocities lead to longer time for runoff to reach the watershed outlet. This may be the direct reason why the GLC prolongs time needed to reach the peak flow rate. Second, hydrological connectivity can affect time to peak flow rate by affecting runoff generation and concentration. According to the results from Meijles and William [75], connecting a topographically higher area to the main channel in a land consolidation procedure had a consequence for the significant increase in the maximum flow and number of peak days, since it improved the connectivity of a watershed, and vice versa. Steep slopes enhance hydrological connectivity, while gentle slopes weaken hydrological connectivity [82]. The GLC weakened the hydrological connectivity by changing the slope gradients of the watershed (Figure 12). Lower hydrological connectivity would trap runoff on hillslopes for a longer time before it flowed to channels [82]. A prolonged time to peak flow rate will provide more time for people, and their properties, to move to safety during severe floods

caused by intensive storms, which are common in the rainy season on the Loess Plateau, China.

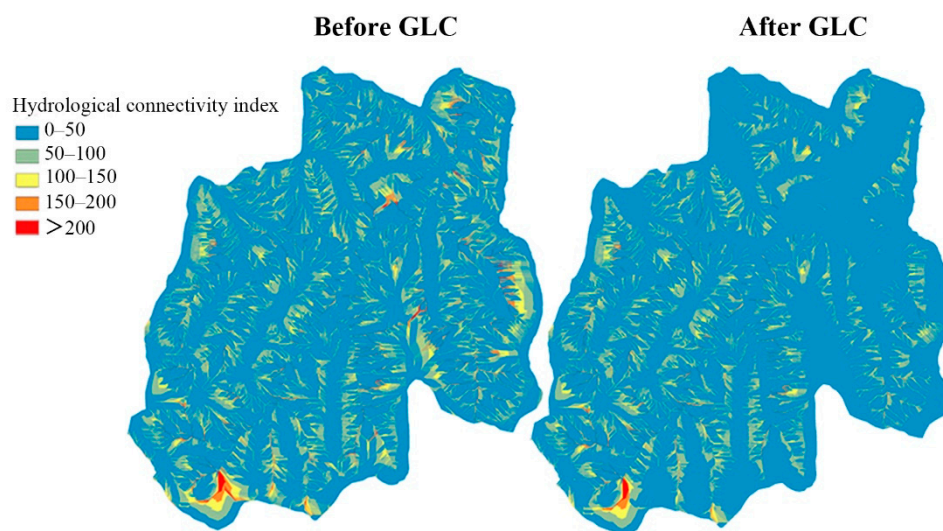


Figure 12. Hydrological connectivity of Xingshuyaozi watershed before GLC (in 2013) and after GLC (in 2019).

4.3. Implication

Land consolidation is a popular way to control flooding and conserve soil and water resources worldwide [83–85]. The current study indicates that GLC provided an effective way to reduce surface runoff and peak flow rate, which are criteria used for flood management, soil and water conservation plans and engineering project design [59]. Enhancing the water retaining ability of the watershed is important for drought and anti-drought management in arid areas such as Loess Plateau. According to IPCC [86], the impact and frequency of water-related crises would be increased due to climate change. Conducting GLC in a rational way is helpful for dealing with water-related crises on Loess Plateau, i.e., flood and drought, which are threatening the local natural system and people's lives.

The span of research on hydrological functioning of GLC on the Loess Plateau is relatively short so far. To provide more useful information on watershed management, the new equilibrium of the hydrological process caused by GLC still needs long-term observation and further study.

5. Conclusions

This study investigated the effects of GLC on runoff and peak flow rate under different rainfall events and hydrological years in the Xingshuyaozi watershed, where the GLC area accounts for 10.36% of the watershed area. In summary, several conclusions are drawn, as follows:

- (1) The GLC reduced mean event surface runoff, and the efficiency in reducing runoff ranged between 6.2% and 24.7%. The highest efficiency of GLC at reducing runoff was found under light rain events. The lowest efficiency of GLC at reducing runoff was found under heavy rain events and the extraordinary storm event.
- (2) After the GLC, the annual surface runoff decreased by 7.63%, 12.04% and 4.45% in the wet year, normal year and dry year, respectively. The order of the GLC's efficiency in reducing annual surface runoff from large to small was as follows: normal year > wet year > dry year.
- (3) The GLC reduced the peak flow rate by 8.1–30.2%. The impact of the GLC on the peak flow rate was greater under light rains than under extraordinary storms. Moreover, the GLC prolonged the time to peak flow rate.
- (4) The GLC affected runoff and peak flow rates by changing slope gradients, hydrological connectivity and land use types.

The results of the current study may provide guidance for the application of the GLC on the Loess Plateau and watershed management in other similar regions.

Author Contributions: Investigation, methodology, software, formal analysis, writing—original draft, writing—review and editing, data curation, visualization, G.W.; conceptualization, methodology, data curation, funding acquisition, investigation, software, supervision, writing—review and editing, S.F.; software, methodology, G.Z.; investigation, validation, C.L. All authors have read and agreed to the published version of the manuscript.

Funding: The research was funded by the National Natural Science Foundation of China (No. 42130701), and the National Key Research and Development Program of China (2017YFD0800502).

Institutional Review Board Statement: Not applicable.

Informed Consent Statement: Not applicable.

Data Availability Statement: The data that support the findings of this study are available from the corresponding author upon reasonable request.

Acknowledgments: All the authors are highly thankful to the reviewers for their fruitful comments to improve the quality of the paper. We thank AJE (<https://www.aje.com/>, accessed on 1 July 2022) for its linguistic assistance during the preparation of this manuscript.

Conflicts of Interest: The authors have no relevant financial or nonfinancial interest to disclose. The authors have no conflict of interest to declare that are relevant to the content of this article. All authors certify that they have no affiliations with or involvement in any organization or entity with any financial interest or nonfinancial interest in the subject matter or materials discussed in this manuscript. The authors have no financial or proprietary interest in any material discussed in this article.

References

- Zhang, Y.; Peng, C.H.; Li, W.Z.; Tian, L.X.; Zhu, Q.Q.; Chen, H.; Fang, X.Q.; Zhang, G.L.; Liu, G.B.; Mu, X.M.; et al. Multiple afforestation programs accelerate the greenness in the ‘Three North’ region of China from 1982 to 2013. *Ecol. Indic.* **2016**, *61*, 404–412. [CrossRef]
- Chen, C.; Park, T.; Wang, X.H.; Piao, S.L.; Xu, B.D.; Chaturvedi, R.K.; Fuchs, R.; Brovkin, V.; Ciais, P.; Fensholt, R.; et al. China and India lead in greening of the world through land-use management. *Nat. Sustain.* **2019**, *2*, 122–129. [CrossRef] [PubMed]
- Gong, J.; Chen, L.; Fu, B.; Huang, Y.; Huang, Z.; Peng, H. Effect of land use on soil nutrients in the Loess Hilly area of the Loess Plateau, China. *Land Degrad. Dev.* **2006**, *17*, 453–465. [CrossRef]
- Xie, C.; Wang, J.N.; Peng, W.; Zhang, K.; Liu, J.J.; Yu, B.C.; Jiang, X.L. The New Round of CCFP: Policy Improvement and Implementation Wisdom—Based on the Results of Social and Economic Benefit Inventory of CCFP in 2015. *For. Econ.* **2016**, *38*, 43–51+81. (In Chinese)
- Bai, L.C.; Wang, N.; Jiao, J.Y.; Chen, Y.X.; Tang, B.Z.; Wang, H.L.; Chen, Y.L.; Yan, X.Q.; Wang, Z.J. Soil erosion and sediment interception by check dams in a watershed for an extreme rainstorm on the Loess Plateau, China. *Int. J. Sediment Res.* **2020**, *35*, 408–416. [CrossRef]
- Ly, Y.H.; Fu, B.J.; Feng, X.M.; Yuan, Z.; Liu, Y.; Chang, R.Y.; Sun, G.; Wu, B.F. A Policy-Driven Large Scale Ecological Restoration: Quantifying Ecosystem Services Changes in the Loess Plateau of China. *PLoS ONE* **2012**, *7*, e31782.
- Wang, S.; Wang, H.Y.; Xie, Y.S.; Luo, H. Evaluation of ecological service function of soil conservation before and after Grain for Green project in Yan’an city. *Res. Soil Water Conserv.* **2019**, *26*, 283–286. (In Chinese)
- Ma, J.F.; Chen, Y.P.; Wang, H.J.; Wang, H.; Wu, J.H.; Su, C.C.; Xu, C. Newly created farmland should be artificially ameliorated to sustain agricultural production on the Loess Plateau. *Land Degrad. Dev.* **2020**, *31*, 2565–2576. [CrossRef]
- Zhao, Y.L.; Wang, Y.Q.; Wang, L.; Zhang, X.Y.; Yu, Y.L.; Jin, Z.; Lin, H.; Chen, Y.P.; Zhou, W.J.; An, Z.S. Exploring the role of land restoration in the spatial patterns of deep soil water at watershed scales. *Catena* **2019**, *172*, 387–396. [CrossRef]
- Bronstert, A.; Vollmer, S.; Ihringer, J. A review of the impact of land consolidation on runoff production and flooding in Germany. *Phys. Chem. Earth* **1995**, *20*, 321–329. [CrossRef]
- Vitikainen, A. An Overview of Land Consolidation in Europe. *Nord. J. Surv. Real Estate Res.* **2004**, *1*, 25–44.
- Liu, S.L.; Dong, Y.H.; Li, D.; Liu, Q.; Wang, J.; Zhang, X.L. Effects of different terrace protection measures in a sloping land consolidation project targeting soil erosion at the slope scale. *Ecol. Eng.* **2013**, *53*, 46–53. [CrossRef]
- Hoeksema, R.J. Three stages in the history of land reclamation in the Netherlands. *Irrig. Drain.* **2007**, *56*, S113–S126. [CrossRef]
- Pašakarnis, G.; Morley, D.; Malienė, V. Rural development and challenges establishing sustainable land use in Eastern European countries. *Land Use Policy* **2013**, *30*, 703–710. [CrossRef]

15. He, M.N.; Wang, Y.Q.; Tong, Y.P.; Zhao, Y.L.; Qiang, X.K.; Song, Y.G.; Wang, L.; Song, Y.; Wang, G.D.; He, C.X. Evaluation of the environmental effects of intensive land consolidation: A field-based case study of the Chinese Loess Plateau. *Land Use Policy* **2020**, *94*, 104523. [[CrossRef](#)]
16. Ishii, A. The methods to consolidate scattered tenanted lots into large rice paddy lots by the land consolidation projects in Japan. *Paddy Water Environ.* **2005**, *3*, 225–233. [[CrossRef](#)]
17. Van den Noort, P.C. Land consolidation in the Netherlands. *Land Use Policy* **1987**, *4*, 11–13. [[CrossRef](#)]
18. Liu, Q.; Wang, Y.Q.; Zhang, J.; Chen, Y.P. Filling Gullies to Create Farmland on the Loess Plateau. *Environ. Sci. Technol.* **2013**, *47*, 7589–7590. [[CrossRef](#)]
19. Zglobicki, W.; Baran-Zglobicka, B.; Gawrysiak, L.; Telecka, M. The impact of permanent gullies on present-day land use and agriculture in loess areas (E. Poland). *Catena* **2015**, *126*, 28–36. [[CrossRef](#)]
20. Zhang, X.C.; Li, Y.R.; Liu, Y.S.; Huang, Y.X.; Wang, Y.S.; Lu, Z. Characteristics and prevention mechanisms of artificial slope instability in the Chinese Loess Plateau. *Catena* **2021**, *207*, 105621. [[CrossRef](#)]
21. Wang, J.; Hu, Y.; Li, P.; Bai, Q.J. Spatial and temporal variations of habitat quality under the background of gully control and land consolidation in Yan'an China. *Acta Ecol. Sin.* **2022**, *42*. (In Chinese)
22. Zhang, X.B.; Jin, Z. Gully land consolidation project in Yan'an is inheritance and development of wrap land dam project on the Loess Plateau. *J. Earth Environ.* **2015**, *6*, 261–264. (In Chinese)
23. Liu, Y.S.; Li, Y.R. Engineering philosophy and design scheme of gully land consolidation in Loess Plateau. *Trans. Chin. Soc. Agric. Eng.* **2017**, *33*, 1–9. (In Chinese)
24. Han, X.L.; Lv, P.Y.; Zhao, S.; Sun, Y.; Yan, S.Y.; Wang, M.H.; Han, X.N.; Wang, X.R. The Effect of the Gully Land Consolidation Project on Soil Erosion and Crop Production on a Typical Watershed in the Loess Plateau. *Land* **2018**, *7*, 113. [[CrossRef](#)]
25. Mihara, M. Effects of agricultural land consolidation on erosion processes in semi-mountainous paddy fields of Japan. *J. Agric. Eng. Res.* **1996**, *64*, 237–247. [[CrossRef](#)]
26. Lou, X.Y.; Gao, J.E.; Han, S.Q.; Guo, Z.H.; Yin, Y. Influence of Land Consolidation Engineering of Gully Channel on Watershed Runoff Yield and Concentration in Loess Hilly and Gully Region. *Water Resour. Power* **2016**, *34*, 23–27. (In Chinese)
27. Sun, P.C.; Gao, J.E.; Han, S.Q.; Yin, Y.; Zhou, M.F. Simulation study on the effects of typical gully land consolidation on runoff-sediment-nitrogen emissions in the loess hilly-gully region. *J. Agro-Environ. Sci.* **2017**, *36*, 1177–1185.
28. Kang, Y.C.; Gao, J.E.; Shao, H.; Zhang, Y.Y.; Li, J.; Gao, Z. Evaluating the flow and sediment effects of gully land consolidation on the Loess Plateau, China. *J. Hydrol.* **2021**, *600*, 126535. [[CrossRef](#)]
29. Guo, Z.H.; Gao, J.N.; Sun, P.C.; Dou, S.H.; Li, J.; Lou, X.Y.; Wang, H.; Ahmad, R.; Gao, Z. Influence of Gully Land Consolidation on Phreatic Water Transformation in the Loess Hilly and Gully Region. *Water* **2021**, *13*, 538. [[CrossRef](#)]
30. Wang, Y.Q.; Sun, H.; Zhao, Y.L. Characterizing spatial-temporal patterns and abrupt changes in deep soil moisture across an intensively managed watershed. *Geoderma* **2019**, *341*, 181–194. [[CrossRef](#)]
31. Wei, W.; Chen, L.D.; Fu, B.J.; Huang, Z.L.; Wu, D.P.; Gui, L.D. The effect of land uses and rainfall regimes on runoff and soil erosion in the semi-arid loess hilly area, China. *J. Hydrol.* **2007**, *335*, 247–258. [[CrossRef](#)]
32. Fang, H.Y. Responses of Runoff and Soil Loss to Rainfall Regimes and Soil Conservation Measures on Cultivated Slopes in a Hilly Region of Northern China. *Int. J. Environ. Res. Public Health* **2021**, *18*, 2102. [[CrossRef](#)]
33. Zheng, H.J.; Nie, X.F.; Liu, Z.; Mo, M.H.; Song, Y.J. Identifying optimal ridge practices under different rainfall types on runoff and soil loss from sloping farmland in a humid subtropical region of Southern China. *Agric. Water Manag.* **2021**, *255*, 107043. [[CrossRef](#)]
34. Lin, Q.T.; Xu, Q.; Wu, F.Q.; Li, T.T. Effects of wheat in regulating runoff and sediment on different slope gradients and under different rainfall intensities. *Catena* **2019**, *183*, 104196. [[CrossRef](#)]
35. Li, Y.S.; Han, S.F.; Wang, Z.H. Soil water properties and its zonation in the Loess Plateau. *Res. Soil Water Conserv.* **1985**, *2*, 1–17. (In Chinese)
36. Xie, B.N.; Jia, X.X.; Qin, Z.F.; Shen, J.; Chang, Q.R. Vegetation dynamics and climate change on the Loess Plateau, China: 1982–2011. *Reg. Environ. Chang.* **2016**, *16*, 1583–1594. [[CrossRef](#)]
37. Chow, V.T.; Maidment, D.R.; Mays, L.W. *Applied Hydrology*; McGraw-Hill, Inc.: New York, USA, 1988.
38. GB/T 28592-2012; Grade of Precipitation. China Meteorological Administration: Beijing, China, 1 August 2012.
39. Rawat, K.S.; Singh, S.K. Estimation of Surface Runoff from Semi-arid Ungauged Agricultural Watershed Using SCS-CN Method and Earth Observation Data Sets. *Water Conserv. Sci. Eng.* **2017**, *1*, 233–247. [[CrossRef](#)]
40. Shi, W.H.; Huang, M.B.; Gongadze, K.; Wu, L.H. A Modified SCS-CN Method Incorporating Storm Duration and Antecedent Soil Moisture Estimation for Runoff Prediction. *Water Resour. Manag.* **2017**, *31*, 1713–1727. [[CrossRef](#)]
41. Nagarajan, N.; Poongothai, S. Spatial Mapping of Runoff from a Watershed Using SCS-CN Method with Remote Sensing and GIS. *J. Hydrol. Eng.* **2012**, *17*, 1268–1277. [[CrossRef](#)]
42. Ajmal, M.; Kim, T.W. Quantifying Excess Stormwater Using SCS-CN-Based Rainfall Runoff Models and Different Curve Number Determination Methods. *J. Irrig. Drain. Eng.* **2015**, *141*, 04014058. [[CrossRef](#)]
43. Al-Juaidi, A.E.M. A simplified GIS-based SCS-CN method for the assessment of land-use change on runoff. *Arab. J. Geosci.* **2018**, *11*, 269.
44. Singh, P.K.; Yaduvanshi, B.K.; Patel, S.; Ray, S. SCS-CN Based Quantification of Potential of Rooftop Catchments and Computation of ASRC for Rainwater Harvesting. *Water Resour. Manag.* **2013**, *27*, 2001–2012. [[CrossRef](#)]

45. Niyazi, B.; Khan, A.A.; Masoud, M.; Elfeki, A.; Basahi, J.; Zaidi, S. Optimum parametrization of the soil conservation service (SCS) method for simulating the hydrological response in arid basins. *Geomat. Nat. Hazards Risk* **2022**, *13*, 1482–1509. [[CrossRef](#)]
46. Yousuf, A.; Bhardwaj, A. Development and application of travel time based gridded runoff and sediment yield model. *Int. J. Environ. Sci. Technol.* **2021**. [[CrossRef](#)]
47. Al-Ghobari, H.; Dewidar, A.; Alataway, A. Estimation of Surface Water Runoff for a Semi-Arid Area Using RS and GIS-Based SCS-CN Method. *Water* **2020**, *12*, 1924. [[CrossRef](#)]
48. Jiao, P.J.; Xu, D.; Wang, S.L.; Yu, Y.D.; Han, S.L. Improved SCS-CN Method Based on Storage and Depletion of Antecedent Daily Precipitation. *Water Resour. Manag.* **2015**, *29*, 4753–4765. [[CrossRef](#)]
49. Jaiswal, R.K.; Yadav, R.N.; Lohani, A.K.; Tiwari, H.L.; Yadav, S. Water balance modeling of Tandula (India) reservoir catchment using SWAT. *Arab. J. Geosci.* **2020**, *13*, 148. [[CrossRef](#)]
50. Knisel, W.G.; Douglas-Mankin, K.R. CREAMS/GLEAMS: Model Use, Calibration, And Validation. *Trans. ASABE* **2012**, *55*, 1291–1302. [[CrossRef](#)]
51. Xiao, B.; Wang, Q.H.; Fan, J.; Han, F.P.; Dai, Q.H. Application of the SCS-CN Model to Runoff Estimation in a Small Watershed with High Spatial Heterogeneity. *Pedosphere* **2011**, *21*, 738–749. [[CrossRef](#)]
52. Fu, S.; Zhang, G.; Wang, N.; Luo, L. Initial Abstraction Ratio In The SCS-CN Method In The Loess Plateau Of China. *Trans. ASABE* **2011**, *54*, 163–169. [[CrossRef](#)]
53. Gao, G.Y.; Fu, B.J.; Lv, Y.H.; Liu, Y.; Wang, S.; Zhou, J. Coupling the modified SCS-CN and RUSLE models to simulate hydrological effects of restoring vegetation in the Loess Plateau of China. *Hydrol. Earth Syst. Sci.* **2012**, *16*, 2347–2364. [[CrossRef](#)]
54. Shi, W.H.; Wang, N.; Wang, M.M.; Li, D.H. Revised runoff curve number for runoff prediction in the Loess Plateau of China. *Hydrol. Process* **2021**, *35*, e14390. [[CrossRef](#)]
55. Soil Conservation Service. Section 4: Hydrology. In *National Engineering Handbook*; US Soil Conservation Service: Washington, DC, USA, 1972.
56. Verma, S.; Singh, P.K.; Mishra, S.K.; Jain, S.K.; Berndtsson, R.; Singh, A.; Verma, R.K. Simplified SMA-inspired 1-parameter SCS-CN model for runoff estimation. *Arab. J. Geosci.* **2018**, *11*, 420. [[CrossRef](#)]
57. Mishra, S.K.; Jain, M.K.; Babu, P.S.; Venugopal, K.; Kaliappan, S. Comparison of AMC-dependent CN-conversion formulae. *Water Resour. Manag.* **2008**, *22*, 1409–1420. [[CrossRef](#)]
58. USDA. *National Engineering Handbook Hydrology Chapters*; USDA: Washington, DC, USA, 1997.
59. Fu, S.H.; Wei, X.; Zhang, G.H. Estimation of peak flows from small watersheds on the Loess Plateau of China. *Hydrol. Processes* **2008**, *22*, 4233–4238. [[CrossRef](#)]
60. United States Department of Agriculture. Chapter 16 Hydrology, National Engineering Handbook. 2007. Available online: <https://www.nrcs.usda.gov/wps/portal/nrcs/detailfull/national/water/manage/hydrology/?cid=stelprdb1043063> (accessed on 1 July 2022).
61. Nash, J.E.; Sutcliffe, J.V. River flow forecasting through conceptual models: Part 1. A discussion of principles. *J. Hydrol.* **1970**, *10*, 282–290. [[CrossRef](#)]
62. Singh, J.; Knapp, H.V.; Arnold, J.G.; Demissie, M. Hydrologic modeling of the Iroquois River watershed using HSPF and SWAT. *J. Am. Water Resour. Assoc.* **2005**, *41*, 343–360. [[CrossRef](#)]
63. Pringle, C.M. Hydrological connectivity and the management of biological reserves: A global perspective. *Ecol. Appl.* **2001**, *11*, 981–998.
64. Bracken, L.J.; Croke, J. The concept of hydrological connectivity and its contribution to understanding runoff-dominated geomorphic systems. *Hydrol. Processes* **2007**, *21*, 1749–1763. [[CrossRef](#)]
65. Moriasi, D. Model evaluation guidelines for systematic quantification of accuracy in watershed simulations. *Trans. ASABE* **2007**, *50*, 885–900. [[CrossRef](#)]
66. Ji, Q.Q.; Gao, Z.; Li, X.Y.; Gao, J.N.; Zhang, G.G.; Ahmad, R.; Liu, G.; Zhang, Y.Y.; Li, W.Z.; Zhou, F.F.; et al. Erosion Transportation Processes as Influenced by Gully Land Consolidation Projects in Highly Managed Small Watersheds in the Loess Hilly-Gully Region; China. *Water* **2021**, *13*, 1540. [[CrossRef](#)]
67. Chaplot, V.A.M.; Bissonnais, Y.L. Runoff features for interrill erosion at different rainfall intensities; slope lengths; and gradients in an agricultural loessial hillslope. *Soil Sci. Soc. Am. J.* **2003**, *67*, 844–851. [[CrossRef](#)]
68. Fox, D.M.; Bryan, R.B.; Price, A.G. The influence of slope angle on final infiltration rate for interrill conditions. *Geoderma* **1997**, *80*, 181–194. [[CrossRef](#)]
69. Zhang, F.M.; Du, L.L.; Yuan, Y.; Wang, S.H.; Guo, S.L. Effects of soil erosion and deposition on soil physical and biochemical properties. *J. Soil Water Conserv.* **2021**, *35*, 161–167. (In Chinese)
70. Zheng, F.L.; Zhang, X.C.; Wang, J.X.; Flanagan, D.C. Assessing applicability of the WEPP hillslope model to steep landscapes in the northern Loess Plateau of China. *Soil Tillage Res.* **2020**, *197*, 104492. [[CrossRef](#)]
71. Wainwright, J.; Parsons, A.J. The effect of temporal variations in rainfall on scale dependency in runoff coefficients. *Water Resour. Res.* **2002**, *38*, 7-1-7-10. [[CrossRef](#)]
72. Jin, Z.; Guo, L.; Wang, Y.Q.; Yu, Y.L.; Lin, H.; Chen, Y.P.; Chu, G.C.; Zhang, J.; Zhang, N.P. Valley reshaping and damming induce water table rise and soil salinization on the Chinese Loess Plateau. *Geoderma* **2019**, *339*, 115–125. [[CrossRef](#)]
73. Yin, X.X.; Chen, L.W.; He, J.D.; Feng, X.Q.; Zeng, W. Characteristics of groundwater flow field after land creation engineering in the hilly and gully area of the Loess Plateau. *Arab. J. Geosci.* **2016**, *9*, 646. [[CrossRef](#)]

74. Evrard, O.; Persoons, E.; Vandaele, K.; van Wesemael, B. Effectiveness of erosion mitigation measures to prevent muddy floods: A case study in the Belgian loam belt. *Agric. Ecosyst. Environ.* **2007**, *118*, 149–158. [[CrossRef](#)]
75. Meijles, E.W.; Williams, A. Observation of regional hydrological response during time periods of shifting policy. *Appl. Geogr.* **2012**, *34*, 456–470. [[CrossRef](#)]
76. Knisel, W.G.E. *CREAMS: A Field Scale Model for Chemicals, Runoff, and Erosion from Agricultural Management Systems*; Conservation Research Report No. 26; Dept. of Agriculture: Washington, DC, USA, 1980.
77. Liu, B.Y.; Wang, D.A.; Fu, S.H.; Cao, W.H. Estimation of Peak Flow Rates for Small Drainage Areas. *Water Resour. Manag.* **2017**, *31*, 1635–1647. [[CrossRef](#)]
78. Wang, Z.L.; Huang, X.H.; Zhang, Z.G.; Niu, Z.H.; Tian, F.X. Experimental Study of Runoff Processes on Bare Loess Hillslope. *Bull. Soil Water Conserv.* **2005**, *4*, 1–4. (In Chinese)
79. Deng, L.Z.; Zhang, L.P.; Fan, X.J.; Wu, Y.H.; Sun, T.Y.; Fei, K. Characteristics of runoff and sediment yield under different rainfall intensities and slope gradients in erosion weather granite area. *Trans. Chin. Soc. Agric. Eng.* **2018**, *34*, 143–150. (In Chinese)
80. Hessel, R. Effects of grid cell size and time step length on simulation results of the Limburg soil erosion model (LISEM). *Hydrol. Processes* **2010**, *19*, 3037–3049. [[CrossRef](#)]
81. Tian, P.; Qiu, H.R.; Feng, Y.; Wu, H.Y.; Wu, T.N. Effects of Rainfall Intensity and Slope Gradient on Runoff and Sediment Production and Erosion Dynamic Process on Red Soil Slope. *Res. Soil Water Conserv.* **2020**, *27*, 106997. (In Chinese)
82. Hooke, J.; Souza, J.; Marchamalo, M. Evaluation of connectivity indices applied to a Mediterranean agricultural catchment. *Catena* **2021**, *207*, 105713. [[CrossRef](#)]
83. Yaslioglu, E.; Arici, I.; Kuscu, H.; Gundogdu, K.S.; Aslan, S.T.A.; Kirmikil, M. Adoption factors of irrigation systems whose projects are synchronized with land consolidation. *Kuwait J. Sci. Eng.* **2008**, *35*, 71–80.
84. Albrecht, J.; Hartmann, T. Land for flood risk management—Instruments and strategies of land management for polders and dike relocations in Germany. *Environ. Sci. Policy* **2021**, *118*, 36–44. [[CrossRef](#)]
85. Caldas, A.M.; Pissarra, T.C.T.; Costa, R.C.A.; Neto, F.C.R.; Zanata, M.; Parahyba, R.D.B.V.; Fernandes, L.F.S.; Pacheco, F.A.L. Flood Vulnerability, Environmental Land Use Conflicts, and Conservation of Soil and Water: A Study in the Batatais SP Municipality, Brazil. *Water* **2018**, *10*, 1357. [[CrossRef](#)]
86. IPCC. *Climate Change 2014: Synthesis Report. Contribution of Working Groups, I, II and III to the Fifth Assessment Report of the Intergovernmental Panel on Climate Change*; IPCC: Geneva, Switzerland, 2014.